MCB
Journals.ASM.org

Macrophage Fusion Is Controlled by the Cytoplasmic Protein Tyrosine Phosphatase PTP-PEST/PTPN12

Inmoo Rhee,[a,b] Dominique Davidson,[a] Cleiton Martins Souza,[a] Jean Vacher,[b,c,d] André Veillette[a,b,d]

Laboratory of Molecular Oncology, Clinical Research Institute of Montréal, Montréal, Québec, Canada[a]; Department of Medicine, McGill University, Montréal, Québec, Canada[b]; Laboratory of Cellular Interactions and Development, Clinical Research Institute of Montréal, Montréal, Québec, Canada[c]; Department of Medicine, University of Montréal, Montréal, Québec, Canada[d]

Macrophages can undergo cell-cell fusion, leading to the formation of multinucleated giant cells and osteoclasts. This process is believed to promote the proteolytic activity of macrophages toward pathogens, foreign bodies, and extracellular matrices. Here, we examined the role of PTP-PEST (PTPN12), a cytoplasmic protein tyrosine phosphatase, in macrophage fusion. Using a macrophage-targeted PTP-PEST-deficient mouse, we determined that PTP-PEST was not needed for macrophage differentiation or cytokine production. However, it was necessary for interleukin-4-induced macrophage fusion into multinucleated giant cells *in vitro*. It was also needed for macrophage fusion following implantation of a foreign body *in vivo*. Moreover, in the RAW264.7 macrophage cell line, PTP-PEST was required for receptor activator of nuclear factor kappa-B ligand (RANKL)-triggered macrophage fusion into osteoclasts. PTP-PEST had no impact on expression of fusion mediators such as β-integrins, E-cadherin, and CD47, which enable macrophages to become fusion competent. However, it was needed for polarization of macrophages, migration induced by the chemokine CC chemokine ligand 2 (CCL2), and integrin-induced spreading, three key events in the fusion process. PTP-PEST deficiency resulted in specific hyperphosphorylation of the protein tyrosine kinase Pyk2 and the adaptor paxillin. Moreover, a fusion defect was induced upon treatment of normal macrophages with a Pyk2 inhibitor. Together, these data argue that macrophage fusion is critically dependent on PTP-PEST. This function is seemingly due to the ability of PTP-PEST to control phosphorylation of Pyk2 and paxillin, thereby regulating cell polarization, migration, and spreading.

Cell-cell fusion is a process by which the membrane, cytoplasm, and nucleus from different cells are combined to form a single multinucleated cell (1–3). It is critical for oocyte fertilization, placental development, muscle cell differentiation, bone resorption, and, possibly, tumor progression. Macrophages (Mϕs) are phagocytic cells involved in the elimination of pathogens, apoptotic cells, senescent red blood cells, and tumor cells (4). They promote tissue repair and wound healing and, paradoxically, can also stimulate tumor growth. Under particular circumstances, Mϕs have the ability to undergo cell-cell fusion, thereby becoming multinucleated giant cells (MGCs) and osteoclasts.

Mϕ fusion is triggered by cytokines such as interleukin-4 (IL-4) and receptor activator of nuclear factor kappa-B ligand (RANKL), which lead to formation of MGCs and osteoclasts, respectively. MGCs were described by Langhans in as early as 1868. They are seen in granulomatous conditions such as tuberculosis, schistosomiasis, and sarcoidosis and following implantation of foreign bodies. They likely play a beneficial role in the elimination of pathogens and foreign bodies (5). However, they may also be detrimental to the host, by promoting tissue destruction and facilitating survival of some pathogens. In contrast, osteoclasts are involved in digestion of bone extracellular matrix and normal bone resorption.

Although the cytokines leading to formation of MGCs and osteoclasts are well-known, the effectors and regulators of Mϕ fusion are still poorly understood (1–3). In both cases, exposure to the triggering cytokine is believed to upregulate expression of fusion mediators like E-cadherin and CD47, which confer the fusion-competent state. Fusion-competent Mϕs then undergo chemotaxis toward each other, followed by cell-cell attachment and, ultimately, membrane fusion and multinucleation.

PTP-PEST (also named PTPN12) is a cytosolic protein tyrosine phosphatase (PTP) (6, 7). It belongs to the PEST (proline-, glutamic acid-, serine-, and threonine-rich) family of PTPs, together with PTPN22 and PTP-HSCF (8). The PTPs are implicated in a wide range of functions, including migration, adhesion, and immune cell activation. PTP-PEST is expressed in nonimmune and immune cells, albeit in the largest amounts in immune cells, including Mϕs. PTP-PEST associates with and dephosphorylates several cytoskeleton-associated proteins, including Cas, paxillin, focal adhesion kinase (FAK), Pyk2, and PSTPIP (9–13). It can also dephosphorylate other types of molecules not associated with the cytoskeleton, such as Shc and various receptor protein tyrosine kinases (PTKs). These multiple interactions are believed to explain the ability of PTP-PEST to regulate several cellular functions, such as migration, adhesion, proliferation, and transformation.

PTP-PEST has been implicated in several cellular processes (8). Analyses of embryo fibroblasts from a constitutive PTP-PEST-deficient mouse and overexpression studies indicated that PTP-PEST is a regulator of cellular adhesion and migration (14–16). It is also needed for normal development of the embryo, as exemplified by the finding that mice lacking PTP-PEST in all cells exhibited embryonic lethality (at embryonic day 10.5) (17). Studies

Received 14 February 2013 **Returned for modification** 6 March 2013
Accepted 5 April 2013
Published ahead of print 15 April 2013
Address correspondence to André Veillette, veillea@ircm.qc.ca.

doi:10.1128/MCB.00197-13

using a conditional PTP-PEST-deficient mouse revealed that this effect is due at least in part to a role of PTP-PEST in endothelial cells during embryonic angiogenesis (18). PTP-PEST is also required for the reactivation of previously activated $CD4^+$ T cells, by promoting homotypic interactions and cytokine exchanges between activated T cells (19). Lastly, PTP-PEST was reported to be a tumor suppressor in human breast cancer and lung cancer, seemingly as a result of its capacity to inhibit the oncogenic potential of activated receptor PTKs (20).

Given the key role of PTP-PEST in cell-cell and cell-substratum interactions (14–16), we addressed its possible involvement in the Mϕ fusion process. We found that PTP-PEST is required for the capacity of Mϕs to fuse into MGCs and osteoclasts. This is seemingly due to a critical role of PTP-PEST in Mϕ polarization, migration, and spreading. This function correlates with the capacity of PTP-PEST to dephosphorylate Pyk2 and regulate paxillin, which also control Mϕ migration and adhesion. Thus, PTP-PEST and, presumably, its substrates, Pyk2 and paxillin, are newly identified key effectors of cell-cell fusion.

MATERIALS AND METHODS

Mice. Mice bearing a conditional allele of the gene encoding PTP-PEST (*Ptpn12*$^{fl/fl}$) were described elsewhere (19). They were backcrossed for at least 12 generations to the C57BL/6 background. To generate mice lacking PTP-PEST in Mϕs, *Ptpn12*$^{fl/fl}$ mice were bred with transgenic mice expressing the Cre recombinase under the control of the *Lys2* promoter (also known as the *LysM* promoter) (Jackson Laboratory, Bar Harbor, ME). Genotyping to detect the floxed (fl) allele and *Cre* was performed as detailed elsewhere (19). In all experiments, littermates were used as controls. All animal experimentation was approved by the IRCM Animal Care Committee and done in accordance with the regulations of the Canadian Council for Animal Care.

Cells. To obtain peritoneal Mϕs, mice were injected intraperitoneally with 4% (wt/vol) thioglycolate broth (BD Biosciences, Mississauga, ON, Canada). After 3 to 4 days, animals were euthanized and Mϕs were collected by peritoneal lavage with ice-cold phosphate-buffered saline (PBS). To obtain bone marrow (BM)-derived Mϕs (BMMϕs), femora and tibiae from mice were flushed with ice-cold Dulbecco modified Eagle medium (DMEM; Invitrogen, Burlington, ON, Canada) containing 10% heat-inactivated fetal bovine serum (FBS; Invitrogen), 100 U/ml penicillin, and 100 μg/ml streptomycin (Invitrogen). Bone marrow cells were then grown in bacterial petri dishes for ~7 days in the presence of tissue culture medium supplemented with 30% (vol/vol) L929 cell conditioned medium as a source of colony-stimulating factor 1 (CSF-1) (21). To obtain splenic Mϕs, spleen tissue was digested using DNase I and Liberase (Roche, Mississauga, ON, Canada). Mϕs were then identified by flow cytometry, using antibodies against CD11b, F4/80, and major histocompatibility complex class II (MHC-II). Granulocytes and monocytes were quantified in BM, by gating on $CD11b^+$ $Ly6G^+$ cells and analyzing expression of CD11b and Ly6C. RAW264.7 cells were obtained from the American Type Culture Collection (Manassas, VA). For downregulation of PTP-PEST expression in RAW264.7 cells, cells were infected with a retrovirus encoding the *Ptpn12*-specific small hairpin RNA (shRNA) expression vector pRS-Puro (Origene, Rockville, MD) following the protocol of the manufacturer. The *Ptpn12*-specific shRNA sequence was GAG ATTCAGTAAGTGCCTTGGAACAATAT. This retrovirus also encodes the puromycin resistance marker, which enables selection of infected cells in puromycin. After single-cell cloning of puromycin-resistant cells, clones showing downregulated PTP-PEST expression were identified by immunoblotting with anti-PTP-PEST antibodies. Pools of three independent clones were used for subsequent experimentation. An irrelevant shRNA-encoding construct provided by the manufacturer was used to generate control cells.

Flow cytometry and antibodies. Cell surface markers were detected by multicolor flow cytometry, according to standard protocols. The following antibodies were used: anti-CD11b (monoclonal antibody [MAb] M1/70), anti-F4/80 (MAb BM8), anti-Ly6C (MAb HK1.4), anti-Ly6G (MAb 1A8), anti-β1 integrin (CD29; MAb HMb1-1), anti-β2 integrin (CD18; MAb M18/2), anti-CD36 (MAb 72-1), anti-SIRPα (CD172a; MAb P84), and anti-CD47 (MAb Miap301). They were purchased from BD Biosciences (Mississauga, ON, Canada), eBioscience (San Diego, CA), or BioLegend (San Diego, CA). Cells were analyzed on a BD Biosciences FACSCalibur flow cytometer using CellQuest software (BD Biosciences). Data were analyzed with FlowJo software (Tree Star Inc., Ashland, OR). Rabbit antibodies against PTP-PEST, Pyk2, Csk, SIRPα, and PSTPIP-1 were generated in our laboratory (12, 19, 22–24). Antiphosphotyrosine MAb 4G10 was obtained from Millipore (Billerica, CA). Antibodies recognizing FAK (catalog no. sc-558), Cas (catalog no. sc-860), STAT-6 (catalog no. sc-981), phospho-STAT-6 (catalog no. sc-11762), arginase 1 (catalog no. sc-271430), E-cadherin (catalog no. 610181), and paxillin (catalog no. 610569) were obtained from Santa Cruz Biotechnology Inc. (Santa Cruz, CA) or BD Transduction Laboratories.

Proliferation and cytokine production assays. BMMϕs (10^4 cells) were seeded in 24-well dishes with complete medium supplemented with L929 cell conditioned medium. Every 2 days, cells were harvested and counted using a hemocytometer. To measure cytokine production, BMMϕs (10^5 cells per well) were stimulated for 24 h in 96-well plates in the presence of the indicated concentrations of lipopolysaccharide (LPS; InvivoGen, Burlington, ON, Canada). Cytokine release in the supernatant was then quantitated using enzyme-linked immunosorbent assay (ELISA) kits, as detailed by the manufacturer (R&D Systems, Burlington, ON, Canada). Assays were performed in triplicate.

Mϕ fusion assays. Mϕ fusion was analyzed as previously described (25). Briefly, peritoneal macrophages were labeled with carboxyfluorescein succinimidyl ester (CFSE) or 5-(and-6)-{[(4-chloromethyl)benzoyl] amino} tetramethylrhodamine (CMTMR) (both from Invitrogen) and then plated on Permanox-coated plastic slides (eight-well Lab-Tek chamber slides; Nunc) in the presence or in the absence of IL-4 (Peprotech, Rocky Hill, NJ). After 48 to 72 h, cells were fixed with 4% paraformaldehyde and stained with DAPI (4′,6-diamidino-2-phenylindole; Vector Laboratories, Burlingame, CA) to detect nuclei. Image analysis was performed with a Zeiss Axioplan fluorescence microscope. Four to five independent images were acquired per well. After subtracting the background, fluorescence was analyzed using MATLAB software (MathWorks, Natick, MA). For induction of MGCs *in vivo*, mice were implanted subcutaneously in the back with round glass coverslips (diameter, 12 mm), as described previously (26). After 4 days, the implants were removed, fixed in methanol, and stained with hematoxylin-eosin (H&E; Sigma). To differentiate RAW264.7 cells into osteoclasts, 2×10^4 cells were cultured in alpha minimum essential medium supplemented with noninactivated 10% FBS (Wisent Inc., St-Bruno, QC, Canada) and RANKL. Culture medium was replaced every 2 days with fresh RANKL-containing complete medium. Cells were then fixed with formaldehyde (EMD Inc., Mississauga, ON, Canada) and processed for staining of tartrate-resistant acid phosphatase (TRAP), as described previously (27). Alternatively, they were stained with DAPI. TRAP-positive cells and DAPI were detected by microscopy. TRAP activity was also measured using a colorimetric assay under linear assay conditions, as detailed by the manufacturer (acid phosphatase assay kit; Abcam, Burlington, ON, Canada).

Pyk2 inhibition. For pharmacological inhibition of Pyk2, cells were incubated for 2 days with the indicated concentrations of the Pyk2/FAK-specific inhibitor PF-431396 (Synkinase, Melbourne, Australia) (28). FcγRI-induced protein tyrosine phosphorylation, tyrosine phosphorylation of Pyk2 and paxillin, and IL-4-triggered fusion were then evaluated.

Migration, spreading, and conjugate formation assays. Migration was analyzed *in vitro* using a Transwell migration apparatus (pore size, 8 μm; Corning, Lowell, MA). Mϕs (1×10^5 cells) in serum-free DMEM were loaded in the upper chamber, while a total of 600 μl serum-free

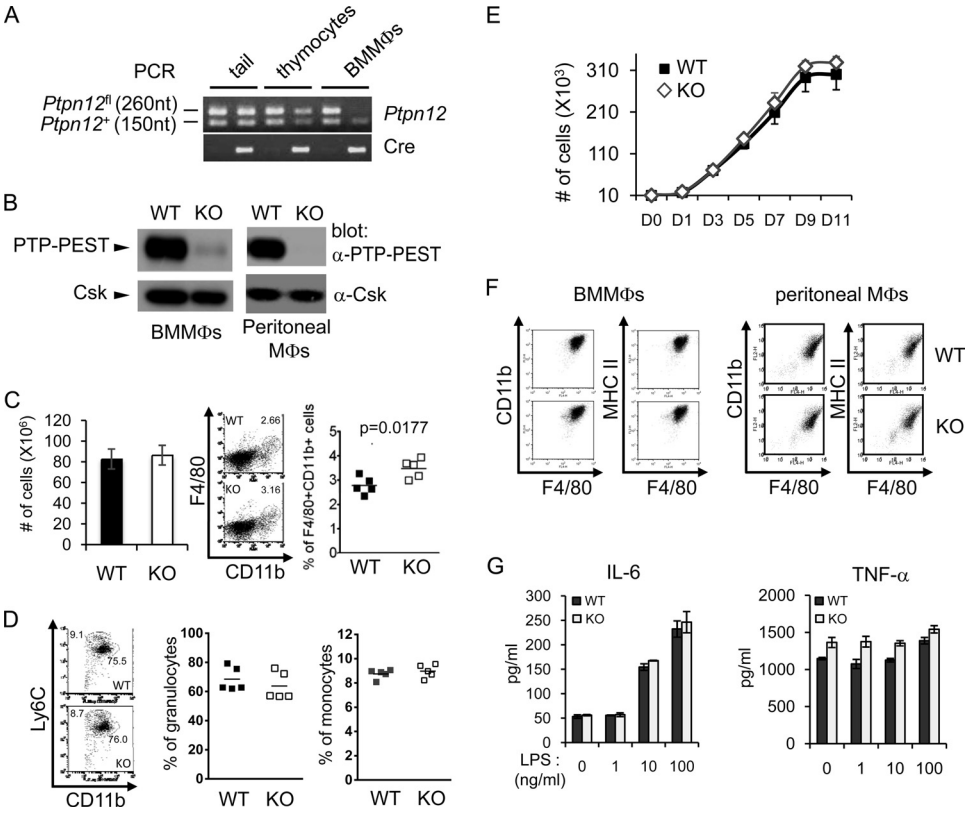

FIG 1 PTP-PEST deficiency in macrophages has no impact on proliferation or differentiation. (A) DNAs from the indicated tissues from *Ptpn12*$^{fl/+}$ *Lys2-Cre*$^{+}$ mice were tested by PCR. Fragments of ~150 and ~260 nucleotides (nt) are expected for the wild-type and floxed alleles, respectively. Deletion of the floxed allele in BMMΦs results in disappearance of the ~260-nucleotide fragment. Representative results of 3 independent experiments are shown. (B) Expression of PTP-PEST protein in BMMΦs and peritoneal Mφs was assessed by immunoblotting of total cell lysates with anti-PTP-PEST antibodies. Csk expression was monitored as a control. Representative results of at least 5 independent experiments are shown. (C) Total splenocyte numbers (left) and proportions of Mφs—defined as CD11b^{+} F4/80^{+} cells—in spleen (middle and right) are shown. For the proportions of Mφs, a representative flow cytometry analysis is shown in the middle, whereas data from 5 independent mice (shown as symbols) are depicted on the right. For total cell numbers, average values from 5 independent mice with standard deviations are shown. For proportions of Mφs, average values are depicted by horizontal lines. Representative results of 3 independent experiments are shown. (D) Granulopoiesis was studied by analyzing CD11b^{+} Ly6G^{+} bone marrow cells for expression of CD11b and Ly6C. Granulocytes are defined as CD11b^{+} Ly6C^{int} cells, whereas monocytes are defined as CD11b^{+} Ly6C^{hi} cells. Dot plot analyses of representative mice are shown on the left. Percentages of granulocytes and monocytes were determined for five independent mice (shown as symbols in the two panels on the right). (E) Proliferation of Mφs in the presence of CSF-1 was assessed. Cells (10^4) were seeded at day 0 (D0). Cell counts were then obtained at the indicated times. Average values from triplicates with standard deviations are shown. Representative results of 3 independent experiments are shown. (F) Expression of Mφ markers on BMMΦs and purified peritoneal Mφs was determined by flow cytometry. Representative results of more than 5 independent experiments are shown. (G) BMMΦs were stimulated for 24 h with the indicated concentrations of LPS. Secretion of IL-6 and tumor necrosis factor alpha (TNF-α) was determined by ELISA. Assays were done in triplicate. Mean values with standard deviations are shown. Under these conditions, production of IL-6 is inducible, whereas that of tumor necrosis factor alpha is constitutive. Representative results of 2 experiments are shown. WT, wild-type mice; KO, knockout mice (mice with PTP-PEST-deficient Mφs).

DMEM with or without chemoattractants (CSF-1, 200 ng/ml; stromal cell-derived factor 1α [SDF-1α], 200 ng/ml; CC chemokine ligand 2 [CCL2], 120 ng/ml; all from Peprotech) was placed in the lower chamber. After 3 h of incubation at 37°C, migrated cells in the lower chamber were harvested and counted by flow cytometry using a flow cytometry absolute count standard (Bangs Laboratories Inc., Fishers, IN). For *in vivo* migration, mice were injected intraperitoneally with thioglycolate, as detailed above. After 2 days, animals were euthanized and Mφs were completely collected by peritoneal lavage with ice-cold PBS. Total numbers of peritoneal cells were assessed. To study cell spreading, BMMΦs were starved of CSF-1 overnight and coverslips were prepared by coating them overnight with fibronectin, collagen, or vitronectin (10 μg/ml; BD Biosciences) at 4°C. On the following day, coverslips were washed with PBS and placed in separate 6-well dishes. CSF-1-deprived Mφs or RAW264.7 cells were harvested and seeded (1×10^5 cells) on the coverslips. After the indicated periods of time at 37°C, Mφs were fixed with 2% paraformaldehyde and mounted on a glass slide for examination by contrast microscopy. Data from 8 to 10 independent fields were acquired. To evaluate conjugate formation, Mφs were labeled with CFSE or CMTMR, as specified above. After labeling, equal numbers of CFSE- and CMTMR-labeled Mφs (2×10^5 cells each) were incubated for the indicated times at 37°C in suspension to induce conjugate formation. To stop the reactions, cells were fixed in paraformaldehyde. Conjugate formation was detected by flow cytometry.

Confocal microscopy. To examine actin filament polarization, BMMΦs (1×10^5 cells) were seeded on glass coverslips and incubated at 37°C for 24 h. After washing with PBS, cells were fixed with 2% paraformaldehyde and permeabilized with 0.2% Triton X-100. Cells were then blocked with 1% bovine serum albumin–PBS at room temperature for 30 min and stained with Alexa Fluor 488-coupled phalloidin (Invitrogen) at room temperature for 30 min. Then, coverslips were washed with PBS and mounted on a glass slide for examination by confocal laser scanning microscopy (Zeiss LSM 710; Carl Zeiss Inc.). Data from 8 to 10 independent fields were acquired. For quantification, an average of 200 cells was counted per staining. In some experiments, cells were plated on glass

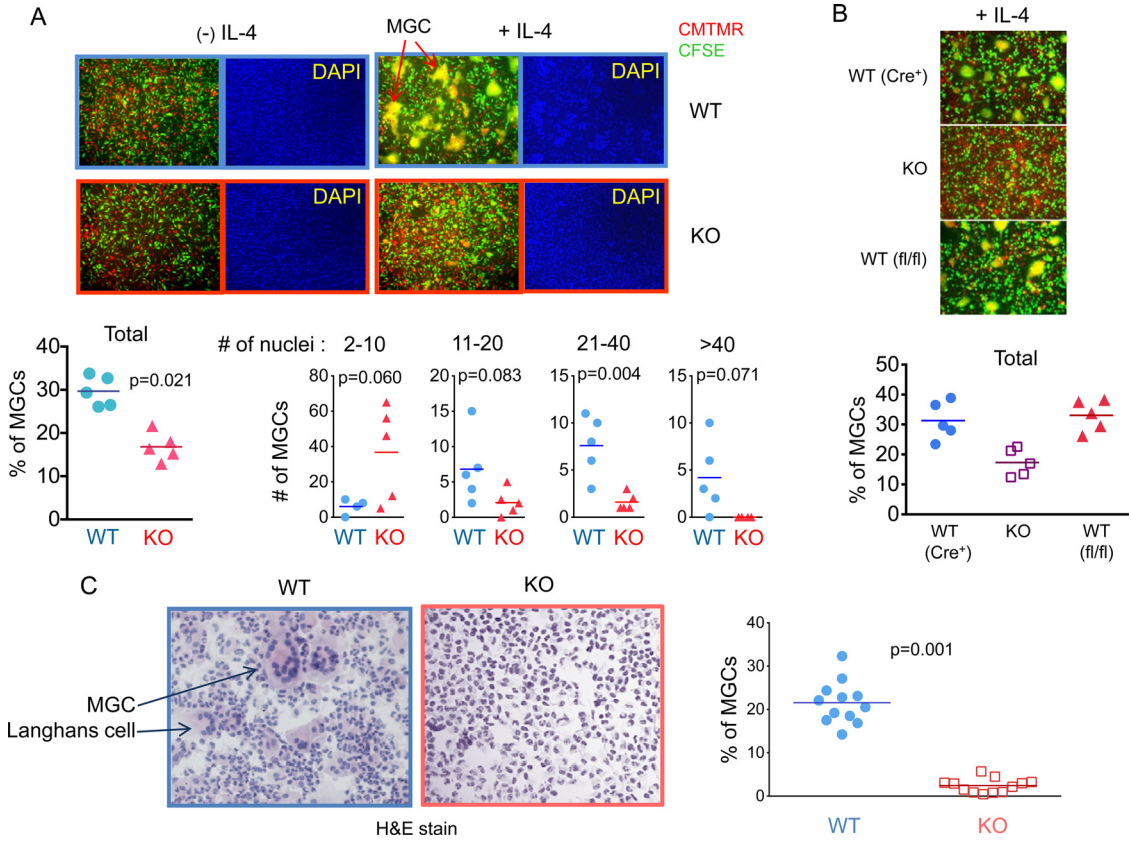

FIG 2 PTP-PEST is necessary for macrophage fusion into multinucleated giant cells *in vitro* and *in vivo*. (A) Fusion *in vitro*. Peritoneal Mϕs were labeled with CFSE (green) or CMTMR (red). They were then mixed and seeded on Permanox slides, in the absence (−) or the presence (+) of IL-4 (10 ng/ml). After 2 to 3 days, cells were stained with DAPI and analyzed by fluorescence microscopy. MGCs are yellow and possess multiple nuclei (examples are indicated by the red arrows). The percentages of MGCs overall and the numbers of MGCs with different ranges of nucleus numbers are shown in the graphs at the bottom. Each symbol represents an independent image field, and average values are shown as horizontal lines. In these experiments, wild-type (WT) controls were *Ptpn12*$^{+/+}$ *Lys2-Cre*$^{+}$ littermates, whereas knockouts were *Ptpn12*$^{fl/fl}$ *Lys2-Cre*$^{+}$ mice. Representative results of 5 independent experiments are shown. (B) An experiment was performed as detailed for panel A, except that both *Ptpn12*$^{+/+}$ *Lys2-Cre*$^{+}$ (wild type [Cre-positive]) and *Ptpn12*$^{fl/fl}$ *Lys2-Cre*$^{-}$ (wild type [fl/fl]) littermates were used as controls. (Top) Representative photographs; (bottom) quantitation of the total numbers of MGCs. (C) Fusion *in vivo*. Glass coverslips were implanted subcutaneously into mice. After 4 days, they were removed and stained with H&E. (Left) A representative coverslip analyzed by light microscopy. MGCs and Langhans cells are shown by arrows. (Right) Percentages of MGCs per total number of cells on the coverslip. Each symbol represents an independent field from a total of three independent mice. Average values are represented by horizontal lines. Representative results of 3 independent experiments are shown. KO, knockout mice (mice with PTP-PEST-deficient Mϕs).

coverslips and starved overnight in CSF-1-free DMEM supplemented with 2% FBS. They were then washed and stimulated or not stimulated for 1 h with recombinant CSF-1 (50 ng/ml), prior to staining with phalloidin.

Immunoprecipitations and immunoblotting. Immunoprecipitations and immunoblotting were performed as outlined elsewhere (29).

Statistical analyses and quantitation. Unpaired Student's *t* tests (two-tailed) were performed using Prism software. Bands in autoradiograms were quantitated using Gel-Pro Analyzer (version 6.0) software (Media Cynernetics, L.P.).

RESULTS

PTP-PEST deficiency has no impact on macrophage differentiation and proliferation. To ascertain the role of PTP-PEST in Mϕ fusion, mice expressing a conditional allele of the PTP-PEST-encoding gene, *Ptpn12*$^{fl/fl}$, were crossed with transgenic mice expressing the Cre recombinase under the control of the lysozyme promoter (*Lys2-Cre* mice; also commonly referred to as *LysM-Cre* mice). This Cre-expressing transgenic mouse enables efficient and specific deletion of target genes in mature Mϕs, as well as in neutrophils (30). In keeping with this, PCR analyses of DNA from heterozygous *Ptpn12*$^{fl/+}$ *Lys2-Cre*$^{+}$ mice showed that the floxed *Ptpn12* allele was deleted in BMMϕs but not in tail tissue or thymocytes (Fig. 1A). To assess the efficiency of PTP-PEST deletion, BMMϕs and thioglycolate-elicited peritoneal Mϕs were obtained from *Ptpn12*$^{fl/fl}$ *Lys2-Cre*$^{+}$ mice (here referred to as PTP-PEST-deficient mice) and *Ptpn12*$^{+/+}$ *Lys2-Cre*$^{+}$ littermate mice (here termed control mice). Immunoblotting of cell lysates with anti-PTP-PEST antibodies showed that Mϕs from *Ptpn12*$^{fl/fl}$ *Lys2-Cre*$^{+}$ mice had a >95% reduction of PTP-PEST expression, in comparison to cells from control mice, indicating that PTP-PEST was efficiently deleted (Fig. 1B).

PTP-PEST deficiency did not interfere with the generation of Mϕs *in vivo* (Fig. 1C). In fact, it caused a modest (~25%) increase in the proportion of Mϕs found in spleen. The basis for this observation is not known. It also did not affect granulopoiesis *in vivo* (Fig. 1D). Lack of PTP-PEST also had no effect on the production of BMMϕs *in vitro*, in response to CSF-1 (Fig. 1E). Furthermore, it had no influence on the expression of CD11b and F4/80, two differentiation markers expressed by mature Mϕs, or on the ex-

pression of MHC-II molecules (Fig. 1F). Lastly, loss of PTP-PEST had no impact on the ability of Mϕs to produce cytokines in response to stimulation of Toll-like receptor 4 (TLR4) by lipopolysaccharide (Fig. 1G). Thus, lack of PTP-PEST had no apparent impact on Mϕ differentiation, proliferation, and cytokine production. The effects of PTP-PEST deficiency on phagocytosis will be described elsewhere.

PTP-PEST is required for macrophage fusion into MGCs. We first examined the ability of PTP-PEST-deficient Mϕs to fuse into MGCs (Fig. 2). This was done because the lysozyme-driven Cre is well expressed in precursors of MGCs but is inconsistently expressed in precursors of osteoclasts. Peritoneal Mϕs from PTP-PEST-deficient or control mice were labeled with CFSE (which exhibits green fluorescence) or CMTMR (which exhibits red fluorescence). They were then mixed and cultured for 3 to 4 days on Permanox-coated slides, in the absence or in the presence of IL-4 (Fig. 2A). Fusion was assessed by detecting cells with yellow fluorescence and by staining nuclei with DAPI. As expected, no Mϕ fusion was observed in the absence of IL-4. However, in the presence of IL-4, Mϕs from control littermate mice exhibited prominent fusion into MGCs. This was true whether *Ptpn12*$^{+/+}$ *Lys2-Cre*$^{+}$ or *Ptpn12*$^{fl/fl}$ *Lys2-Cre*$^{-}$ mice were used as controls (Fig. 2B). In contrast, PTP-PEST-deficient Mϕs had markedly reduced fusion efficiency (Fig. 2A and B). Both the number of MGCs and the number of nuclei per MGC were severely diminished.

We also tested the ability of Mϕs to fuse into MGCs *in vivo*, in response to implantation of a foreign body (Fig. 2C). To this end, glass coverslips were implanted subcutaneously into the back of control or PTP-PEST-deficient mice. After 4 days, coverslips were removed and stained with H&E. Control mice exhibited a prominent accumulation of MGCs on the coverslip. They also showed formation of Langhans giant cells, a variant of fused Mϕs classically found under granulomatous conditions and characterized by the horseshoe-like distribution of nuclei (31). In comparison, however, PTP-PEST-deficient mice had a near absence of MGCs and Langhans cells. Hence, PTP-PEST was necessary for Mϕs to fuse into MGCs *in vitro* and *in vivo*.

PTP-PEST is necessary for fusion of the RAW264.7 macrophage cell line into osteoclasts. Expression of Cre utilizing any of the promoters tested so far has been inconsistent at deleting conditionally targeted genes in osteoclasts. Therefore, to ascertain the role of PTP-PEST in osteoclast formation, we took an alternative approach using the mouse Mϕ cell line RAW264.7, which differentiates into osteoclast-like cells in response to RANKL (Fig. 3). RAW264.7-derived osteoclasts share many of the characteristics of bone marrow-derived osteoclasts (32). First, RAW264.7 cells were infected with retroviruses encoding a PTP-PEST-specific shRNA or an irrelevant shRNA. Puromycin-resistant clones were selected and tested for PTP-PEST expression. Pools of clones were then used for experimentation. PTP-PEST expression was reduced by >90% in cells bearing the PTP-PEST shRNA, in comparison to control cells (Fig. 3A). Then, cells were treated or not treated with RANKL, and osteoclast formation was monitored by staining with DAPI and by assaying for TRAP, a marker of osteoclast differentiation (Fig. 3B and C). The formation of multinucleated cells and induction of TRAP in response to RANKL were severely compromised in RAW264.7 cells lacking PTP-PEST, in comparison to control cells (Fig. 3B and C).

These results support the idea that PTP-PEST is also required for Mϕ fusion into osteoclasts. Furthermore, they indicate that the impact on Mϕ fusion seen in Fig. 2 is not due to an effect of PTP-PEST deficiency in other cell types, such as neutrophils, but rather is caused by a macrophage-intrinsic effect.

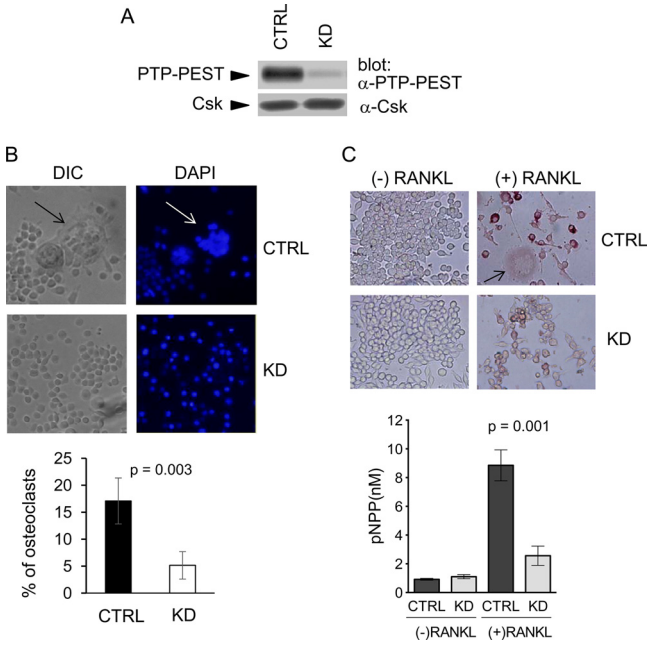

FIG 3 PTP-PEST is needed for macrophage fusion into osteoclasts. Cells of the Mϕ cell line RAW264.7 were transduced with retroviruses encoding a PTP-PEST-specific shRNA or an irrelevant shRNA. (A) Expression of PTP-PEST was assessed by immunoblotting of total cell lysates with anti-PTP-PEST antibodies. Csk expression was monitored as a control. Representative results of 3 independent experiments are shown. (B) Cells were treated or not treated with RANKL. RANKL-stimulated cells were stained with DAPI and analyzed by differential interference contrast (DIC) microscopy and fluorescence microscopy. The percentage of RANKL-stimulated cells forming osteoclasts was quantitated in 5 independent fields (bottom). Average values with standard deviations are shown. The arrows indicate osteoclast-like cells. (C) After 5 days, they were also fixed and stained for TRAP (purple) (top). A typical osteoclast is shown by the arrow. TRAP activity was also quantitated using a colorimetric assay (bottom). Representative results of 4 independent experiments are shown. CTRL, control cells transduced with irrelevant shRNA; KD, knockdown cells transduced with PTP-PEST-specific shRNA; pNPP, *para*-nitrophenylphosphate.

PTP-PEST is not needed for induction of fusion mediators. To determine how PTP-PEST promoted fusion, we first focused on the proximal events of the fusogenic cascade (Fig. 4). The IL-4 receptor (IL-4R) is a member of the cytokine receptor family which primarily functions by activating the Jak-STAT pathways (33). The major immediate effector of IL-4R is the transcription factor STAT-6, which stimulates transcription of several of the fusion mediators. Immunoblotting with a phosphorylation-specific antibody against activated STAT-6 showed that PTP-PEST deficiency had no effect on the ability of IL-4 to trigger tyrosine phosphorylation of STAT-6 (Fig. 4A).

The ability of IL-4 to induce expression of fusion mediators was also tested (Fig. 4B and C). The latter include β1 integrins, β2 integrins, E-cadherin, CD36, CD47, dendritic cell (DC)-derived protein DC-STAMP, and matrix metallopeptidase 9 (MMP-9). Flow cytometry studies showed that a lack of PTP-PEST had no influence on baseline expression of β1 integrins, β2 integrins, E-cadherin, CD36, and CD47 (Fig. 4B). It also had no impact on the

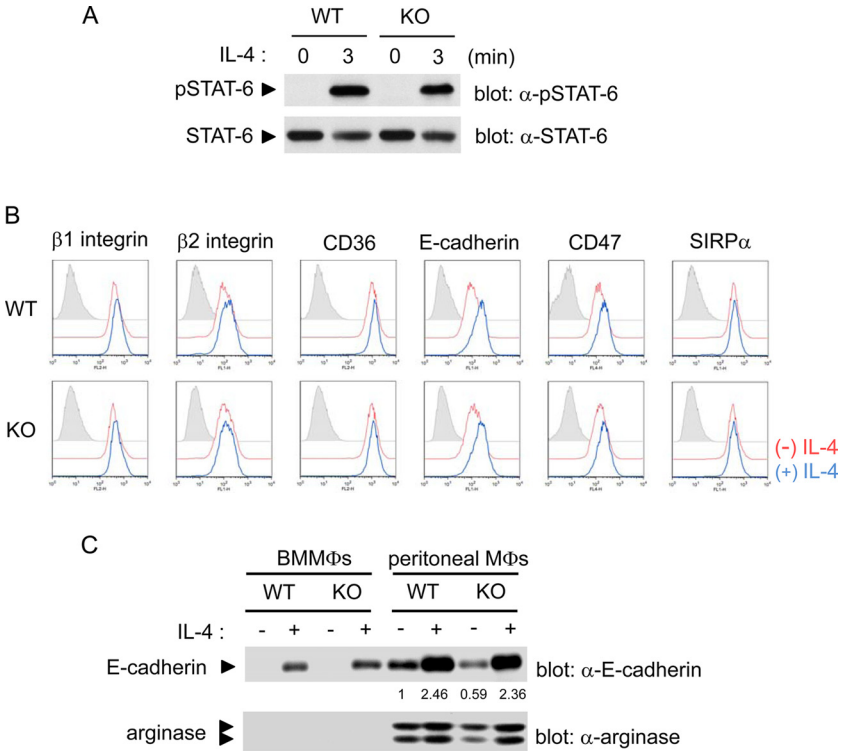

FIG 4 Normal induction of fusion mediators by PTP-PEST-deficient macrophages. (A) Peritoneal Mϕs were stimulated or not stimulated with IL-4 (10 ng/ml) for the indicated times. Cells were then lysed and probed by immunoblotting with phosphorylation-specific antibodies against STAT-6 (top) or antibodies directed against all STAT-6 molecules (bottom). Representative results of 3 independent experiments are shown. (B) As in panel A, except that cells were treated or not treated with IL-4 for 24 h. They were then stained with antibodies against the indicated cell surface molecules. Staining with isotype control antibodies is depicted by the filled gray curves. Representative results of 3 independent experiments are shown. (C) As in panel B, except that cells were lysed and probed by immunoblotting with antibodies against E-cadherin or arginase. Quantitation of the data for E-cadherin is shown below the top panel. Data are the abundance relative to the abundance of E-cadherin in unstimulated wild-type cells. Representative results of 3 independent experiments are shown. WT, wild-type mice; KO, knockout mice (mice with PTP-PEST-deficient Mϕs).

capacity of IL-4 to augment expression of some of these receptors. The lack of an effect on E-cadherin expression was confirmed by immunoblotting with anti-E-cadherin antibodies (Fig. 4C).

In addition to triggering fusion, IL-4 can induce Mϕ differentiation into alternatively activated Mϕs, which are involved in tissue repair and immunosuppression (34). To address if PTP-PEST influenced the generation of alternatively activated Mϕs by IL-4, the induction of arginase, a marker of alternative activation, was evaluated (Fig. 4C). Arginase induction by IL-4 was not affected by PTP-PEST deficiency. Thus, PTP-PEST was not required for proximal IL-4R signaling, induction of fusion mediators, or IL-4-evoked differentiation into alternatively activated Mϕs.

PTP-PEST promotes macrophage actin rearrangement, chemotaxis, and spreading. Since the induction of fusion mediators was not influenced by PTP-PEST, we examined the subsequent events implicated in the fusion process (Fig. 5). Previous studies showed that the ability of fusion-competent Mϕs to migrate toward each other in response to chemokines, in particular, CCL2, was critical for fusion (35, 36). Using a Transwell migration assay, we observed that PTP-PEST deficiency markedly compromised the capacity of Mϕs to migrate in response to CCL2 (Fig. 5A). This was also true for chemotaxis induced by another chemokine, SDF-1α, and by the growth factor CSF-1. Likewise, PTP-PEST deficiency resulted in diminished Mϕ migration *in vivo*, during thioglycolate-elicited peritonitis (Fig. 5B).

Fusion also requires the ability of neighboring Mϕs to attach to each other, in order to juxtapose the cellular membranes (1–3, 37–39). This adhesion is largely mediated by E-cadherin, which bridges cell-cell contacts (37–39). To test the influence of PTP-PEST on the ability of Mϕs to adhere to each other, a cell conjugation assay was performed (Fig. 5C). Mϕs were labeled with either CFSE or CMTMR and were incubated in suspension for various periods of time. Cells were then fixed, and conjugate formation was detected by flow cytometry. The ability of PTP-PEST-deficient Mϕs to form conjugates was only minimally reduced in comparison to that of control Mϕs.

Spreading is an integrin-initiated response in which cells flatten upon plating on an integrin ligand-coated adhesive surface (40). Thus, to evaluate the role of PTP-PEST in cell-substratum interactions, we tested the capacity of Mϕs to spread on glass coverslips coated with various ligands for integrins (Fig. 5D). The ability of Mϕs lacking PTP-PEST to spread in response to fibronectin, collagen, and vitronectin was severely reduced. A smaller fraction of PTP-PEST-deficient cells underwent full spreading, and greater proportions underwent partial spreading or did not spread. This was true for all three integrin ligands.

We also tested the impact of PTP-PEST deficiency on the ability of RAW264.7 cells to undergo migration and spread (Fig. 6). As was the case for primary macrophages, PTP-PEST deficiency in RAW264.7 cells resulted in compromised chemotaxis in response

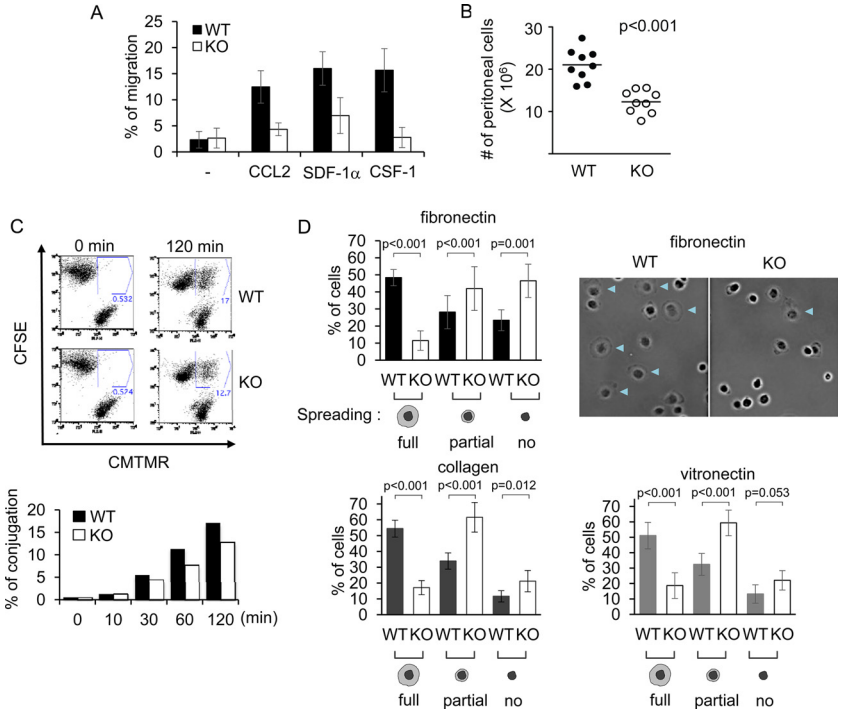

FIG 5 PTP-PEST is required for macrophage migration and spreading. (A) The ability of peritoneal Mϕs to migrate *in vitro* was tested in a Transwell migration assay (pore size, 8 μm). Mϕs were placed in the upper chamber, whereas the chemoattractants were placed in the lower chamber. After 3 h, the number of peritoneal Mϕs migrating into the lower chamber was ascertained by flow cytometry, as detailed in Materials and Methods. Average values with standard deviations from three independent experiments are shown. Representative results of 3 independent experiments are shown. (B) The capacity of Mϕs to migrate *in vivo* was analyzed by injection of thioglycolate into the peritoneal cavity. After 2 days, the number of Mϕs in the peritoneal cavity was determined by flow cytometry. Symbols represent individual mice. Average values are shown as horizontal bars. Representative results of 4 independent experiments are shown. (C) Peritoneal Mϕs were labeled with CFSE or CMTMR. They were then mixed 1:1 and incubated for the indicated times at 37°C. Cells were then fixed, and conjugate formation was assessed by flow cytometry. Conjugates (boxed) are cell aggregates showing dual staining for CFSE and CMTMR. Percentages of conjugate formation are shown at the right of each panel. Data are represented graphically at the bottom. Representative results of 3 independent experiments are shown. (D) BMMϕs were seeded at 37°C on coverslips coated with the indicated ligands for integrins. After 10 min, cells were fixed and analyzed by microscopy. Representative fields for the assay using fibronectin are shown at the top right. Arrowheads indicate cells showing full spreading. Quantitation of the data from 8 to 10 independent fields is presented at the top left and at the bottom. Average values with standard deviations are shown. Schematic representations of the appearance of cells showing full, partial, or no spreading are depicted. Representative results of 3 independent experiments are shown.

to CCL2, SDF-1α, and serum (Fig. 6A). Likewise, it caused decreased spreading on fibronectin (Fig. 6B).

Actin organization was analyzed using confocal microscopy (Fig. 7). BMMϕs were plated on glass coverslips, and actin filaments were detected by staining of permeabilized cells with phalloidin, which detects actin filaments (Fig. 7A). As described elsewhere (41, 42), control Mϕs had a heterogeneous morphology. However, many cells exhibited flattening of their body and a broad leading edge. They also exhibited multiple long filopodia. Approximately 20 to 25% of cells had a polarized appearance, i.e., a preferential accumulation of actin filaments at one edge of the cell. In contrast, PTP-PEST-deficient Mϕs were more elongated and frequently bipolar. They also had very few filopodia. Lastly, only ~10% of these cells exhibited a polarized appearance. The impact of CSF-1 on actin organization was also examined (Fig. 7B). For this purpose, BMMϕs were deprived of CSF-1 overnight and then incubated or not incubated for 1 h with CSF-1. Addition of CSF-1 resulted in a prominent increase of the number of control Mϕs having membrane protrusions known as lamellipodia. This was also the case for PTP-PEST-deficient cells, although a small decrease in the frequency of lamellipodium formation was noted. Lamellipodia are proposed to help directional mobility during cell migration.

Hence, PTP-PEST played a critical role in the ability of Mϕs to rearrange their actin cytoskeleton, undergo chemotaxis, and spread on a substratum.

PTP-PEST regulates Pyk2 and paxillin in macrophages. Next, we wanted to identify the intracellular tyrosine phosphorylation substrates through which PTP-PEST influenced Mϕ fusion (Fig. 8). Since a lack of PTP-PEST compromised Mϕ polarization, migration, and adhesion, we focused on PTP-PEST substrates known to influence these processes. The extent of tyrosine phosphorylation of the substrates was examined by antiphosphotyrosine immunoblotting (Fig. 8A). Tyrosine phosphorylation of the PTK Pyk2 and the adaptor paxillin was increased 3- to 5-fold in PTP-PEST-deficient Mϕs compared to control Mϕs. These two proteins are key regulators of cell migration, adhesion, and spreading (43, 44). Little or no expression of FAK and Cas was detected in these cells. The effect on tyrosine phosphorylation of Pyk2 was constitutive, being seen both in the absence and in the presence of IL-4 (Fig. 8B). In contrast, there was no increase in the extent of tyrosine phosphorylation of PSTPIP-1 and SIRPα. A selective increase in tyrosine phosphorylation of Pyk2 and, to a lesser extent, paxillin was also seen in PTP-PEST-deficient RAW264.7 cells (Fig. 8C). Although FAK was detectably expressed in RAW264.7 cells, no effect on FAK tyrosine phosphorylation

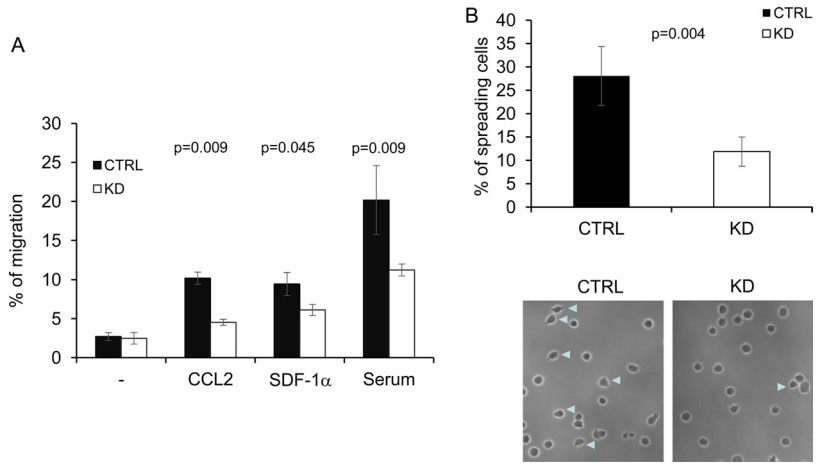

FIG 6 Altered migration and adhesion in PTP-PEST-deficient RAW264.7 cells. (A) The ability of RAW264.7 cells to migrate *in vitro* was tested in a Transwell migration assay (pore size, 8 μm). Mϕs were placed in the upper chamber, whereas the chemoattractants were placed in the lower chamber. After 3 h, the number of Mϕs migrating into the lower chamber was ascertained by flow cytometry, as detailed in Materials and Methods. Representative results of 3 independent experiments are shown. (B) RAW264.7 cells were seeded at 37°C on coverslips coated with fibronectin. After 30 min, cells were fixed and analyzed by microscopy. Representative fields for the assay using fibronectin are shown on the right. Quantitation of the data from 8 to 10 independent fields is presented on the left. Average values with standard deviations are shown. Arrowheads indicate cells with spreading. Representative results of 3 independent experiments are shown. CTRL, control cells transduced with irrelevant shRNA; KD, knockdown cells transduced with PTP-PEST-specific shRNA.

was observed in these cells. Therefore, PTP-PEST was required for dephosphorylation of Pyk2 and paxillin.

Pyk2 activity is required for macrophage fusion. To ascertain the possible impact of dysregulation of Pyk2 on fusion, we tested the effect of a pharmacological inhibitor of this PTK, PF-431396 (Fig. 9) (28, 45–47). This inhibitor was reported to be efficient at suppressing the kinase activity of Pyk2 *in vitro* (50% inhibitory concentration, 31 nM). To ensure that PF-431396 was specific for

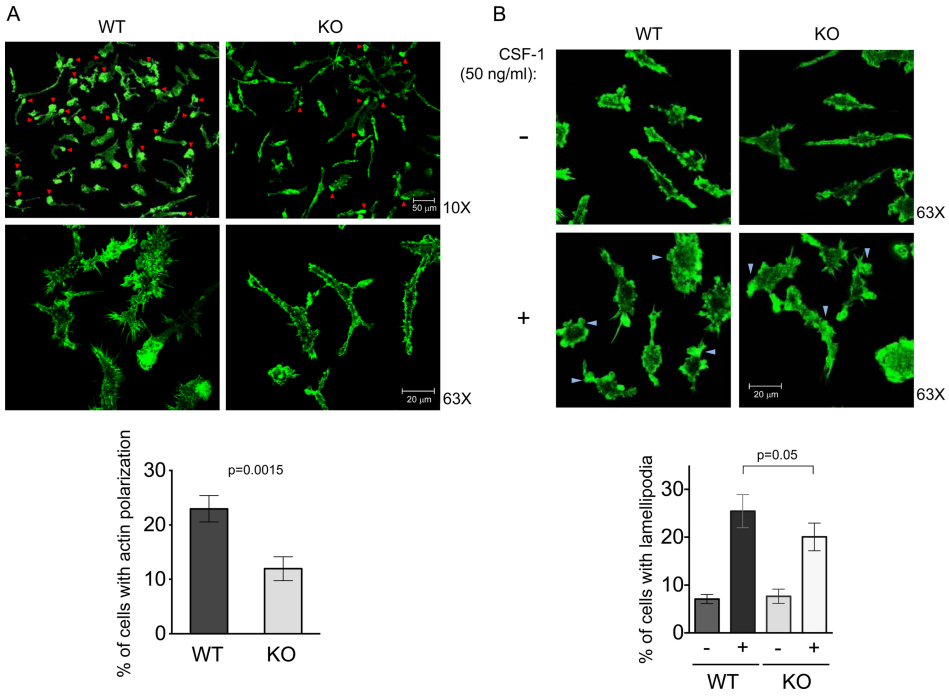

FIG 7 Altered polarization of actin filaments in PTP-PEST-deficient macrophages. (A) BMMϕs were plated on glass coverslips, fixed, and stained with Alexa Fluor 488-conjugated phalloidin to visualize actin filaments. Immunofluorescence was analyzed by confocal laser scanning microscopy (top). Two different magnifications are shown. Polarized cells (arrowheads) are defined as cells in which the actin filaments are concentrated at one edge of the cell. Quantification of actin polarization from 8 to 10 independent fields is presented (bottom). Average values with standard deviations are shown. (B) Cells were plated as described for panel A and starved overnight in CSF-1-free DMEM containing 2% fetal bovine serum. They were then stimulated or not stimulated for 1 h with recombinant CSF-1 (50 ng/ml). Actin rearrangement was analyzed as detailed for panel A. Immunofluorescence analyses are depicted at the top. Percentages of cells showing lamellipodia are shown at the bottom. Lamellipodia are indicated by arrowheads. WT, wild-type mice; KO, knockout mice (mice with PTP-PEST-deficient Mϕs).

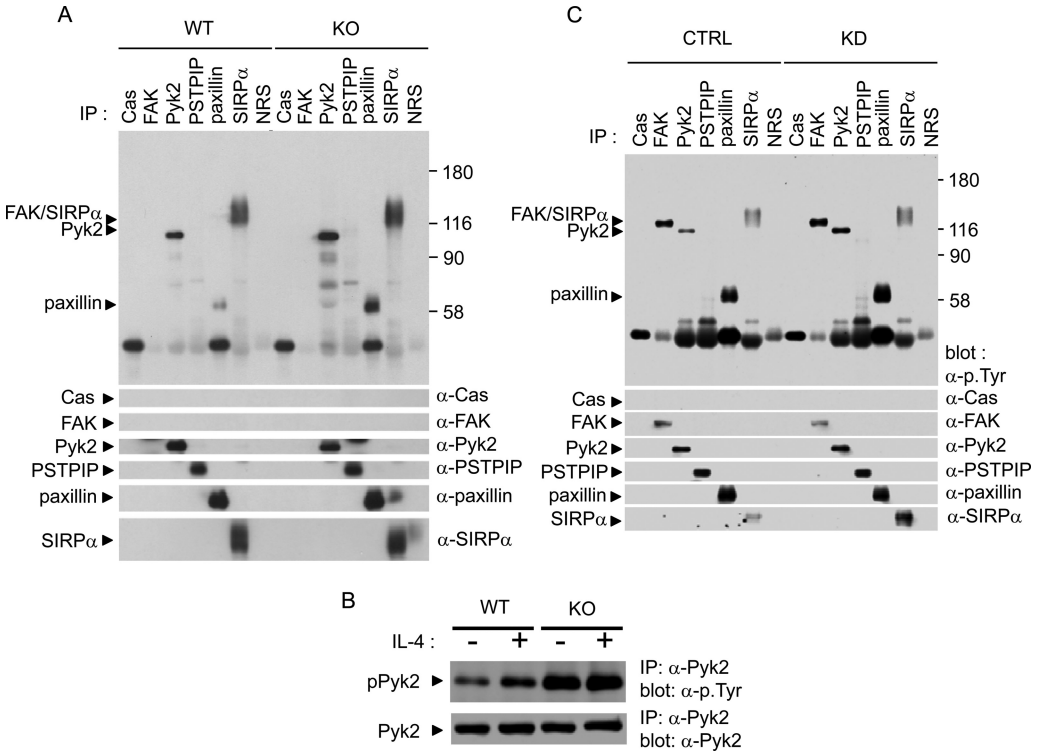

FIG 8 Altered protein tyrosine phosphorylation in PTP-PEST-deficient macrophages. (A) The extent of tyrosine phosphorylation of the indicated substrates in primary mouse Mϕs was analyzed by immunoprecipitation (IP) with substrate-specific antibodies, followed by immunoblotting with antiphosphotyrosine (α-p.Tyr) antibodies. The presence of the substrates in the immunoprecipitates was confirmed by reprobing the membranes with the indicated antibodies. Note that these Mϕs did not detectably express Cas and expressed little or no FAK. Representative results of 4 independent experiments are shown. NRS, normal rabbit serum. (B) Tyrosine phosphorylation of Pyk2 was determined in peritoneal Mϕs, stimulated or not stimulated with IL-4. Representative results of 3 independent experiments are shown. (C) The extent of tyrosine phosphorylation of the indicated substrates in RAW264.7 cells was analyzed as detailed for panel A. Representative results of 5 independent experiments are shown. WT, wild-type mice; KO, knockout mice (mice with PTP-PEST-deficient Mϕs); CTRL, control cells transduced with irrelevant shRNA; KD, knockdown cells transduced with PTP-PEST-specific shRNA.

Pyk2 in Mϕs, its impact on overall protein tyrosine phosphorylation was first analyzed (Fig. 9A). PF-431396 had no effect on the ability to trigger protein tyrosine phosphorylation upon engagement of the high-affinity Fc receptor for IgG, FcγRI. Since FcγRI is coupled to Src and Syk family PTKs in Mϕs, this observation implied that PF-431396 was not inhibiting the functions of Src and Syk PTKs in these cells. In contrast, PF-431396 inhibited the extent of tyrosine phosphorylation of Pyk2 and paxillin (Fig. 9B). A partial decrease in the abundance of Pyk2 was seen, as is frequently observed with other PTKs inactivated by chemical inhibitors. Nonetheless, the diminution of Pyk2 tyrosine phosphorylation was more marked than the decrease in its abundance, implying that the intrinsic activity and autophosphorylation of Pyk2 were also suppressed. Paxillin is known to bind and be a substrate of Pyk2 (46, 48).

Next, Mϕs from control mice were incubated with various concentrations of PF-431396, and IL-4-induced fusion was evaluated (Fig. 9C). Treatment of control Mϕs with PF-431396 resulted in a dose-dependent abrogation of IL-4-induced Mϕ fusion. The inhibitor also suppressed the residual IL-4-induced fusion observed in PTP-PEST-deficient Mϕs. Thus, the kinase activity of Pyk2 was needed for Mϕ fusion.

DISCUSSION

In this study, we examined the role of PTP-PEST in Mϕ fusion, using a conditional PTP-PEST-deficient mouse. PTP-PEST had no appreciable impact on Mϕ differentiation *in vitro* or *in vivo*, the proliferative response of Mϕs to CSF-1 *in vitro*, or TLR4-mediated cytokine production. However, it was required for the capacity of peritoneal Mϕs to fuse into MGCs in response to IL-4 *in vitro*. Likewise, it was necessary for the ability of Mϕs to form MGCs and Langhans cells, following implantation of a foreign body (glass coverslip) *in vivo*. It was also needed for the aptitude of RAW264.7 cells to fuse into osteoclasts after exposure to RANKL *in vitro*. Unfortunately, PTP-PEST appeared to be inefficiently deleted in osteoclast precursors from *Ptpn12*$^{fl/fl}$ *Lys2-Cre*$^{+}$ mice, precluding a valid analysis of osteoclast formation *in vivo* (data not shown). Nonetheless, on the basis of our data with RAW264.7 cells, it seems probable that PTP-PEST is also needed for osteoclast fusion.

Previous studies showed that several sequential steps are implicated in Mϕ fusion. They include, in order, (i) induction of fusion mediators, (ii) cell polarization, chemokine-triggered migration, and integrin-mediated adhesion, (iii) cell-cell attachment, and (iv) cell fusion and multinucleation. PTP-PEST-deficient peritoneal Mϕs had no appreciable defect in IL-4-induced upregulation of fusion mediators, including the adhesion molecules E-cadherins and β integrins, indicating that the proximal fusogenic cascade was not regulated by PTP-PEST (Fig. 10). This is unlike other regulators of protein tyrosine phosphorylation, such as the receptors TREM-2 and OSCAR, the adaptors DAP12

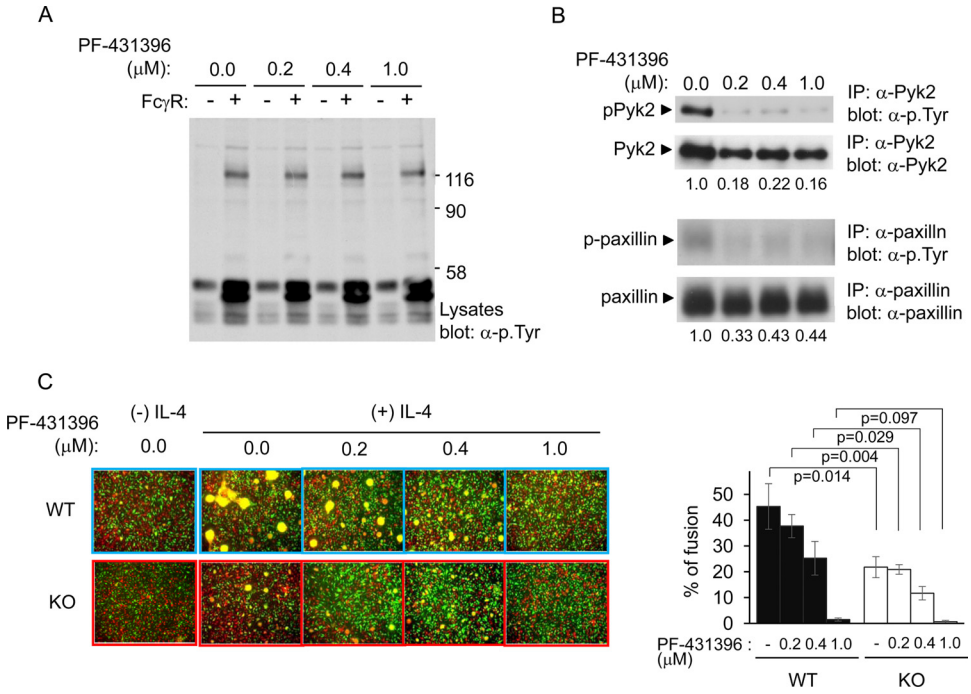

FIG 9 The activity of Pyk2 is required for macrophage fusion. (A) Peritoneal macrophages were incubated or not incubated for 2 days with the indicated concentrations of PF-431396. Cells were then washed and stimulated (+) or not stimulated (−) for 2 min with a mouse IgG2a antibody (MAb 7G7), a high-affinity ligand for FcγRI. After lysis, phosphotyrosine-containing proteins were detected by immunoblotting with antiphosphotyrosine (α-p.Tyr) antibodies. Representative results of 2 independent experiments are shown. (B) Cells were treated with PF-431396 as detailed for panel A but were not stimulated with IgG2a. After cell lysis, the indicated substrates were recovered by immunoprecipitation and probed by antiphosphotyrosine immunoblotting. Relative tyrosine phosphorylation of the substrates (shown at the bottom) was calculated by quantifying the bands in the antiphosphotyrosine immunoblots and correcting for the total amounts of protein detected in the immunoblots with antibodies against the individual substrates. (C) Peritoneal Mϕs from wild-type (WT) mice or PTP-PEST-deficient (knockout [KO]) mice were labeled and processed for macrophage fusion assay as detailed in the legend to Fig. 2, with the exception that cells were treated or not treated with the indicated concentrations of the Pyk2 inhibitor PF-431396. After 2 to 3 days, cells were analyzed by fluorescence microscopy (left). MGCs are yellow. Quantitation of the data is shown on the right. Five independent microscope fields were used for quantitation. Representative results of 3 independent experiments are shown.

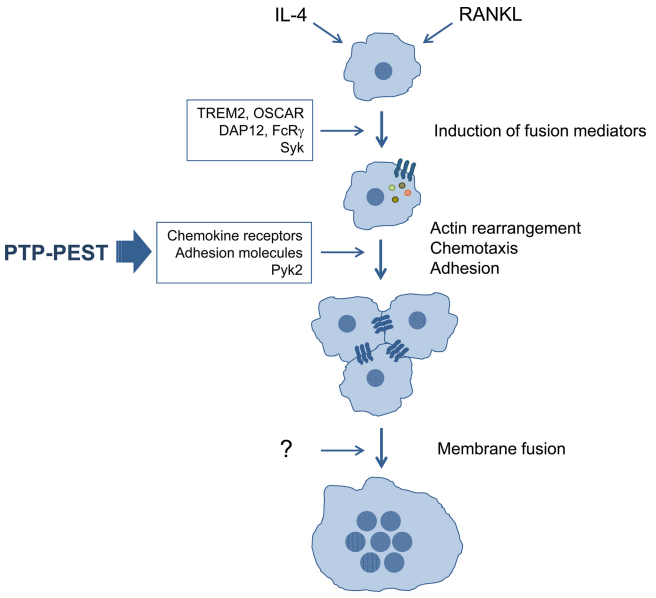

FIG 10 Role of PTP-PEST in macrophage fusion. PTP-PEST is required for the ability of macrophages to fuse into multinucleated giant cells and osteoclasts. This is due to a role of PTP-PEST in the control of polarization, chemokine-induced migration, and integrin-triggered adhesion. The roles of some of the other signaling molecules implicated in macrophage fusion are also indicated. See Discussion for further details.

and FcRγ, and the PTK Syk, which control Mϕ fusion by influencing expression of fusion mediators (49).

Although PTP-PEST deficiency had no effect on the proximal fusogenic cascade, PTP-PEST-deficient mouse Mϕs exhibited compromised polarization of actin filaments. They also exhibited reduced migration in response to CCL2, a chemokine involved in Mϕ fusion (35, 36). In addition, they had a diminished aptitude to spread on surfaces coated with the integrin ligands fibronectin, collagen, and vitronectin. Integrin-mediated adhesion to extracellular matrix is also known to promote Mϕ fusion (36, 50). Therefore, we believe that PTP-PEST promoted Mϕ fusion into MGCs by stimulating actin rearrangement, chemotaxis, and integrin-mediated adhesion (Fig. 10). As defects in chemokine-induced migration and integrin-triggered spreading were also seen in PTP-PEST-deficient RAW264.7 cells, it seems probable that this mechanism also explains the ability of PTP-PEST to promote fusion into osteoclasts.

PTP-PEST deficiency resulted in enhanced tyrosine phosphorylation of a specific set of intracellular proteins in Mϕs. In peritoneal Mϕs, BMMϕs, and RAW264.7 cells, it yielded augmented tyrosine phosphorylation of Pyk2 and paxillin. These effects were constitutive, being seen in the absence of any added stimulation. They were not amplified by addition of IL-4. No effect on other substrates, such as PSTPIP-1 and SIRPα, was observed. This profile was distinct from the profiles previously observed in PTP-

PEST-deficient fibroblasts, T cells, and endothelial cells, in which hyperphosphorylation of Cas, paxillin, FAK, and PSTPIP-1, hyperphosphorylation of Pyk2, and hyperphosphorylation of Cas and FAK, respectively, was observed (11, 16, 18, 19). Thus, the substrates regulated by PTP-PEST vary from one cell type to the other. This may reflect divergences in the expression patterns of the substrates.

The only substrate having a known catalytic activity and showing enhanced tyrosine phosphorylation in PTP-PEST-deficient mouse Mϕs and RAW264.7 cells was Pyk2. Experiments with a pharmacological inhibitor of Pyk2, PF-431396, showed that this inhibitor resulted in a dose-dependent suppression of IL-4-triggered fusion by normal Mϕs. This was accompanied by suppression of tyrosine phosphorylation of paxillin, an adaptor implicated in the control of cell migration and adhesion (44). Hence, the enzymatic function of Pyk2, perhaps through phosphorylation of paxillin, appeared to be necessary for Mϕ fusion.

It might seem paradoxical that the inhibition of Pyk2 activity caused by PF-431396 and the augmentation of Pyk2 activity induced by PTP-PEST deficiency had the same inhibitory impact on Mϕ fusion. However, these convergent effects are not unheard of. Another eloquent example was reported for PTP-PEST-deficient fibroblasts (13, 16). These cells exhibited enhanced tyrosine phosphorylation of Cas, FAK, and paxillin that was accompanied by a migration defect. Paradoxically, fibroblasts lacking either of these PTP-PEST-regulated substrates also had a migration defect (16, 44, 51, 52). Thus, lack or inhibition of a substrate can have the same deleterious impact on migration as constitutive enhancement of tyrosine phosphorylation of this substrate. This is presumably because both alterations cause a spatiotemporal dysregulation of the migration machinery that results in altered migration.

In summary, the data reported herein showed that the phosphatase PTP-PEST is an essential regulator of Mϕ fusion into MGCs and osteoclasts. This effect does not relate to the ability to influence expression of fusion mediators in response to fusion-inducing cytokines. Rather, it correlates with the ability of PTP-PEST to control actin rearrangement, chemokine-triggered migration, and integrin-induced adhesion, seemingly through Pyk2 and, perhaps, paxillin. These findings contribute to a better understanding of the Mϕ fusion process. The ability of eukaryotic cells to undergo fusion is a highly conserved process (1–3). It is also critical for many other events, such as oocyte fertilization and muscle cell differentiation. Given the broad expression of PTP-PEST in mammalian cells, it is tempting to speculate that PTP-PEST may also have a crucial role in these other fusion processes.

ACKNOWLEDGMENTS

We thank the members of our laboratories for discussions. We also thank Cheolho Cheong for advice.

This work was supported by grants from the Canadian Institutes of Health Research and the Canadian Cancer Society Research Institute to A.V. and J.V. A.V. holds the Canada Research Chair in Signaling in the Immune System.

REFERENCES

1. **Helming L, Gordon S.** 2009. Molecular mediators of macrophage fusion. Trends Cell Biol. **19**:514–522.
2. **Vignery A.** 2008. Macrophage fusion: molecular mechanisms. Methods Mol. Biol. **475**:149–161.
3. **McNally AK, Anderson JM.** 2011. Macrophage fusion and multinucleated giant cells of inflammation. Adv. Exp. Med. Biol. **713**:97–111.
4. **Murphy K, Travers P, Walport M, Janeway C.** 2008. Immunobiology, 7th ed. Garland Science, New York, NY.
5. **Lay G, Poquet Y, Salek-Peyron P, Puissegur MP, Botanch C, Bon H, Levillain F, Duteyrat JL, Emile JF, Altare F.** 2007. Langhans giant cells from M. tuberculosis-induced human granulomas cannot mediate mycobacterial uptake. J. Pathol. **211**:76–85.
6. **Yang Q, Co D, Sommercorn J, Tonks NK.** 1993. Cloning and expression of PTP-PEST. A novel, human, nontransmembrane protein tyrosine phosphatase. J. Biol. Chem. **268**:17650.
7. **Charest A, Wagner J, Muise ES, Heng HH, Tremblay ML.** 1995. Structure of the murine MPTP-PEST gene: genomic organization and chromosomal mapping. Genomics **28**:501–507.
8. **Veillette A, Rhee I, Souza CM, Davidson D.** 2009. PEST family phosphatases in immunity, autoimmunity, and autoinflammatory disorders. Immunol. Rev. **228**:312–324.
9. **Garton AJ, Flint AJ, Tonks NK.** 1996. Identification of p130(cas) as a substrate for the cytosolic protein tyrosine phosphatase PTP-PEST. Mol. Cell. Biol. **16**:6408–6418.
10. **Davidson D, Cloutier JF, Gregorieff A, Veillette A.** 1997. Inhibitory tyrosine protein kinase p50csk is associated with protein-tyrosine phosphatase PTP-PEST in hemopoietic and non-hemopoietic cells. J. Biol. Chem. **272**:23455–23462.
11. **Cote JF, Charest A, Wagner J, Tremblay ML.** 1998. Combination of gene targeting and substrate trapping to identify substrates of protein tyrosine phosphatases using PTP-PEST as a model. Biochemistry **37**:13128–13137.
12. **Shen Y, Schneider G, Cloutier JF, Veillette A, Schaller MD.** 1998. Direct association of protein-tyrosine phosphatase PTP-PEST with paxillin. J. Biol. Chem. **273**:6474–6481.
13. **Cote JF, Chung PL, Theberge JF, Halle M, Spencer S, Lasky LA, Tremblay ML.** 2002. PSTPIP is a substrate of PTP-PEST and serves as a scaffold guiding PTP-PEST toward a specific dephosphorylation of WASP. J. Biol. Chem. **277**:2973–2986.
14. **Garton AJ, Tonks NK.** 1999. Regulation of fibroblast motility by the protein tyrosine phosphatase PTP-PEST. J. Biol. Chem. **274**:3811–3818.
15. **Sastry SK, Lyons PD, Schaller MD, Burridge K.** 2002. PTP-PEST controls motility through regulation of Rac1. J. Cell Sci. **115**:4305–4316.
16. **Angers-Loustau A, Cote JF, Charest A, Dowbenko D, Spencer S, Lasky LA, Tremblay ML.** 1999. Protein tyrosine phosphatase-PEST regulates focal adhesion disassembly, migration, and cytokinesis in fibroblasts. J. Cell Biol. **144**:1019–1031.
17. **Sirois J, Cote JF, Charest A, Uetani N, Bourdeau A, Duncan SA, Daniels E, Tremblay ML.** 2006. Essential function of PTP-PEST during mouse embryonic vascularization, mesenchyme formation, neurogenesis and early liver development. Mech. Dev. **123**:869–880.
18. **Souza CM, Davidson D, Rhee I, Gratton JP, Davis EC, Veillette A.** 2012. The phosphatase PTP-PEST/PTPN12 regulates endothelial cell migration and adhesion, but not permeability, and controls vascular development and embryonic viability. J. Biol. Chem. **287**:43180–43190.
19. **Davidson D, Shi X, Zhong MC, Rhee I, Veillette A.** 2010. The phosphatase PTP-PEST promotes secondary T cell responses by dephosphorylating the protein tyrosine kinase Pyk2. Immunity **33**:167–180.
20. **Sun T, Aceto N, Meerbrey KL, Kessler JD, Zhou C, Migliaccio I, Nguyen DX, Pavlova NN, Botero M, Huang J, Bernardi RJ, Schmitt E, Hu G, Li MZ, Dephoure N, Gygi SP, Rao M, Creighton CJ, Hilsenbeck SG, Shaw CA, Muzny D, Gibbs RA, Wheeler DA, Osborne CK, Schiff R, Bentires-Alj M, Elledge SJ, Westbrook TF.** 2011. Activation of multiple proto-oncogenic tyrosine kinases in breast cancer via loss of the PTPN12 phosphatase. Cell **144**:703–718.
21. **Hume DA, Gordon S.** 1983. Optimal conditions for proliferation of bone marrow-derived mouse macrophages in culture: the roles of CSF-1, serum, Ca^{2+}, and adherence. J. Cell. Physiol. **117**:189–194.
22. **Davidson D, Veillette A.** 2001. PTP-PEST, a scaffold protein tyrosine phosphatase, negatively regulates lymphocyte activation by targeting a unique set of substrates. EMBO J. **20**:3414–3426.
23. **Cloutier JF, Veillette A.** 1996. Association of inhibitory tyrosine protein kinase p50csk with protein tyrosine phosphatase PEP in T cells and other hemopoietic cells. EMBO J. **15**:4909–4918.
24. **Veillette A, Thibaudeau E, Latour S.** 1998. High expression of inhibitory

receptor SHPS-1 and its association with protein-tyrosine phosphatase SHP-1 in macrophages. J. Biol. Chem. **273**:22719–22728.
25. **Helming L, Gordon S.** 2007. Macrophage fusion induced by IL-4 alternative activation is a multistage process involving multiple target molecules. Eur. J. Immunol. **37**:33–42.
26. **Ryan GB, Spector WG.** 1970. Macrophage turnover in inflamed connective tissue. Proc. R. Soc. Lond. B Biol. Sci. **174**:269–292.
27. **Ferron M, Boudiffa M, Arsenault M, Rached M, Pata M, Giroux S, Elfassihi L, Kisseleva M, Majerus PW, Rousseau F, Vacher J.** 2011. Inositol polyphosphate 4-phosphatase B as a regulator of bone mass in mice and humans. Cell Metab. **14**:466–477.
28. **Buckbinder L, Crawford DT, Qi H, Ke HZ, Olson LM, Long KR, Bonnette PC, Baumann AP, Hambor JE, Grasser WA, III, Pan LC, Owen TA, Luzzio MJ, Hulford CA, Gebhard DF, Paralkar VM, Simmons HA, Kath JC, Roberts WG, Smock SL, Guzman-Perez A, Brown TA, Li M.** 2007. Proline-rich tyrosine kinase 2 regulates osteoprogenitor cells and bone formation, and offers an anabolic treatment approach for osteoporosis. Proc. Natl. Acad. Sci. U. S. A. **104**:10619–10624.
29. **Veillette A, Bookman MA, Horak EM, Bolen JB.** 1988. The CD4 and CD8 T cell surface antigens are associated with the internal membrane tyrosine-protein kinase p56lck. Cell **55**:301–308.
30. **Goren I, Allmann N, Yogev N, Schurmann C, Linke A, Holdener M, Waisman A, Pfeilschifter J, Frank S.** 2009. A transgenic mouse model of inducible macrophage depletion: effects of diphtheria toxin-driven lysozyme M-specific cell lineage ablation on wound inflammatory, angiogenic, and contractive processes. Am. J. Pathol. **175**:132–147.
31. **Anderson JM.** 2000. Multinucleated giant cells. Curr. Opin. Hematol. **7**:40–47.
32. **Collin-Osdoby P, Osdoby P.** 2012. RANKL-mediated osteoclast formation from murine RAW 264.7 cells. Methods Mol. Biol. **816**:187–202.
33. **Schindler C, Levy DE, Decker T.** 2007. JAK-STAT signaling: from interferons to cytokines. J. Biol. Chem. **282**:20059–20063.
34. **Gordon S, Martinez FO.** 2010. Alternative activation of macrophages: mechanism and functions. Immunity **32**:593–604.
35. **Kyriakides TR, Foster MJ, Keeney GE, Tsai A, Giachelli CM, Clark-Lewis I, Rollins BJ, Bornstein P.** 2004. The CC chemokine ligand, CCL2/MCP1, participates in macrophage fusion and foreign body giant cell formation. Am. J. Pathol. **165**:2157–2166.
36. **McNally AK, Anderson JM.** 2002. Beta1 and beta2 integrins mediate adhesion during macrophage fusion and multinucleated foreign body giant cell formation. Am. J. Pathol. **160**:621–630.
37. **Skokos EA, Charokopos A, Khan K, Wanjala J, Kyriakides TR.** 2011. Lack of TNF-alpha-induced MMP-9 production and abnormal E-cadherin redistribution associated with compromised fusion in MCP-1-null macrophages. Am. J. Pathol. **178**:2311–2321.
38. **Van den Bossche J, Bogaert P, van Hengel J, Guerin CJ, Berx G, Movahedi K, Van den Bergh R, Pereira-Fernandes A, Geuns JM, Pircher H, Dorny P, Grooten J, De Baetselier P, Van Ginderachter JA.** 2009. Alternatively activated macrophages engage in homotypic and heterotypic interactions through IL-4 and polyamine-induced E-cadherin/catenin complexes. Blood **114**:4664–4674.
39. **Moreno JL, Mikhailenko I, Tondravi MM, Keegan AD.** 2007. IL-4 promotes the formation of multinucleated giant cells from macrophage precursors by a STAT6-dependent, homotypic mechanism: contribution of E-cadherin. J. Leukoc. Biol. **82**:1542–1553.
40. **Frame M, Norman J.** 2008. A tal(in) of cell spreading. Nat. Cell Biol. **10**:1017–1019.
41. **Wells CM, Walmsley M, Ooi S, Tybulewicz V, Ridley AJ.** 2004. Rac1-deficient macrophages exhibit defects in cell spreading and membrane ruffling but not migration. J. Cell Sci. **117**:1259–1268.
42. **Bhavsar PJ, Vigorito E, Turner M, Ridley AJ.** 2009. Vav GEFs regulate macrophage morphology and adhesion-induced Rac and Rho activation. Exp. Cell Res. **315**:3345–3358.
43. **Avraham H, Park SY, Schinkmann K, Avraham S.** 2000. RAFTK/Pyk2-mediated cellular signalling. Cell. Signal. **12**:123–133.
44. **Hagel M, George EL, Kim A, Tamimi R, Opitz SL, Turner CE, Imamoto A, Thomas SM.** 2002. The adaptor protein paxillin is essential for normal development in the mouse and is a critical transducer of fibronectin signaling. Mol. Cell. Biol. **22**:901–915.
45. **Tse KW, Dang-Lawson M, Lee RL, Vong D, Bulic A, Buckbinder L, Gold MR.** 2009. B cell receptor-induced phosphorylation of Pyk2 and focal adhesion kinase involves integrins and the Rap GTPases and is required for B cell spreading. J. Biol. Chem. **284**:22865–22877.
46. **Bonnette PC, Robinson BS, Silva JC, Stokes MP, Brosius AD, Baumann A, Buckbinder L.** 2010. Phosphoproteomic characterization of PYK2 signaling pathways involved in osteogenesis. J. Proteomics **73**:1306–1320.
47. **Guimaraes CR, Rai BK, Munchhof MJ, Liu S, Wang J, Bhattacharya SK, Buckbinder L.** 2011. Understanding the impact of the P-loop conformation on kinase selectivity. J. Chem. Inf. Model. **51**:1199–1204.
48. **Li X, Earp HS.** 1997. Paxillin is tyrosine-phosphorylated by and preferentially associates with the calcium-dependent tyrosine kinase in rat liver epithelial cells. J. Biol. Chem. **272**:14341–14348.
49. **Helming L, Tomasello E, Kyriakides TR, Martinez FO, Takai T, Gordon S, Vivier E.** 2008. Essential role of DAP12 signaling in macrophage programming into a fusion-competent state. Sci. Signal. **1**:ra11. doi:10.1126/scisignal.1159665.
50. **Takeda Y, Tachibana I, Miyado K, Kobayashi M, Miyazaki T, Funakoshi T, Kimura H, Yamane H, Saito Y, Goto H, Yoneda T, Yoshida M, Kumagai T, Osaki T, Hayashi S, Kawase I, Mekada E.** 2003. Tetraspanins CD9 and CD81 function to prevent the fusion of mononuclear phagocytes. J. Cell Biol. **161**:945–956.
51. **Honda H, Nakamoto T, Sakai R, Hirai H.** 1999. p130(Cas), an assembling molecule of actin filaments, promotes cell movement, cell migration, and cell spreading in fibroblasts. Biochem. Biophys. Res. Commun. **262**:25–30.
52. **Ilic D, Furuta Y, Kanazawa S, Takeda N, Sobue K, Nakatsuji N, Nomura S, Fujimoto J, Okada M, Yamamoto T.** 1995. Reduced cell motility and enhanced focal adhesion contact formation in cells from FAK-deficient mice. Nature **377**:539–544.